Supporting Information

Silicone Oil Induced Spontaneous *Single-crystal-to-Single-Crystal* Phase Transitions in Ethynyl substituted *ortho* and *meta*-fluorinated benzamides

Subhrajyoti Bhandary[a], *Deepak Chopra*[a*]

[a]*Crystallography and Crystal Chemistry Laboratory, Department of Chemistry, Indian Institute of Science Education and Research Bhopal, Bhopal By-Pass Road, Bhopal, Madhya Pradesh, India-462066.*

Email: dchopra@iiserb.ac.in; Fax: 91-0755-6691311

Synthesis and Materials

The compounds *ortho* and *meta* were synthesized and characterized by ^{1}H NMR (see below). Silicone oil (Polydimethyl Siloxane, Kinetic Viscosity- 300 cS, Weight per *ml* at 20 □C- around 0.970 g) were purchased form SDFCL (S D fine-Chem Limited) Company, India and directly used for experiments. The ^{1}H NMR spectrum of Silicone oil is shown in Figure S1c.

General Procedure of Synthesis

One equivalent of 3-aminophenyl acetylene was taken in a round bottomed flask containing dry dichloromethane and put on a magnetic stirrer. The mixture was then cooled to 0 °C followed by addition of 1.5 equivalent of triethyl amine. The fluoro substituted benzoyl chloride (1.2 equivalent) was then added drop wise to the reaction mixture with constant stirring under inert N_2 atmosphere. The completion of the reaction was monitored with thin layer chromatography. At the end, reaction mixture was extracted by dichloromethane solvent and product was purified by column chromatography.

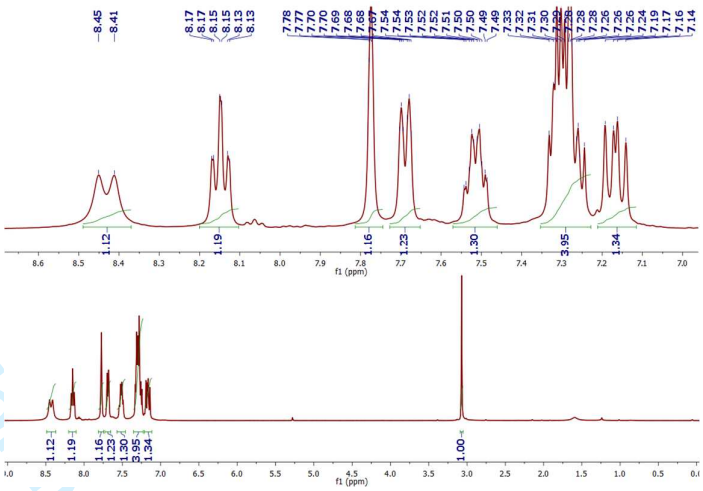

Figure S1a. ^{1}H-NMR spectra of the synthesized *ortho* compound in $CDCl_3$.

N*-(3-Ethynylphenyl)-2-fluorobenzamide: *ortho

Yield = 95%, M. P. = 76 ºC, FTIR (cm^{-1}): 3295 (N-H), 1666 (C=O); ^{1}H-NMR ($CDCl_3$, 400 MHz): δ 8.43 (d, 1H), 8.15 (t, J = 8.08 Hz, 1H), 7.78 (s, 1H), 7.69 (d, J = 7.90 Hz, 1H), 7.51 (m, 1H), 7.29 (m, 3H), 7.17 (m, 1H), 3.07 (s, 1H) .

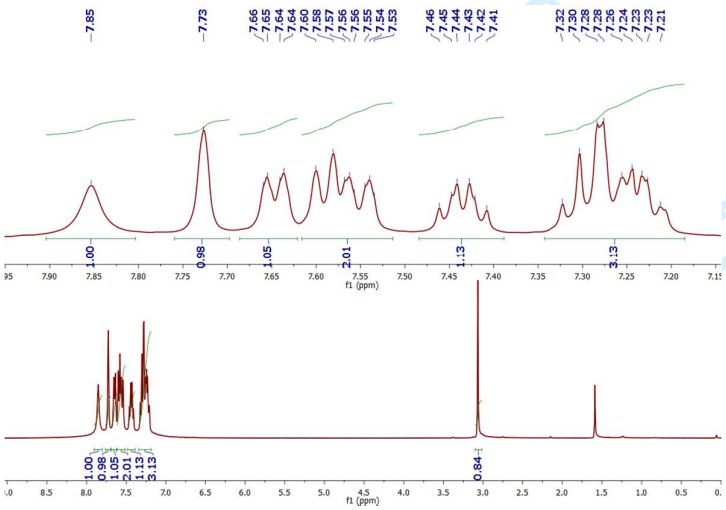

Figure S1b. ^{1}H-NMR spectra of the synthesized *meta* compound in $CDCl_3$.

N*-(3-Ethynylphenyl)-3-fluorobenzamide: *meta

Yield = 97%, M. P. = 103 ºC, FTIR (cm^{-1}): 3298 (N-H), 1651 (C=O); ^{1}H-NMR ($CDCl_3$, 400 MHz): δ 7.85 (s, 1H), 7.73 (s, 1H), 7.65 (d, J = 7.64 Hz, 1H), 7.57 (m, 2H), 7.43 (m, 1H), 7.26 (m, 3H), 3.07 (s, 1H).

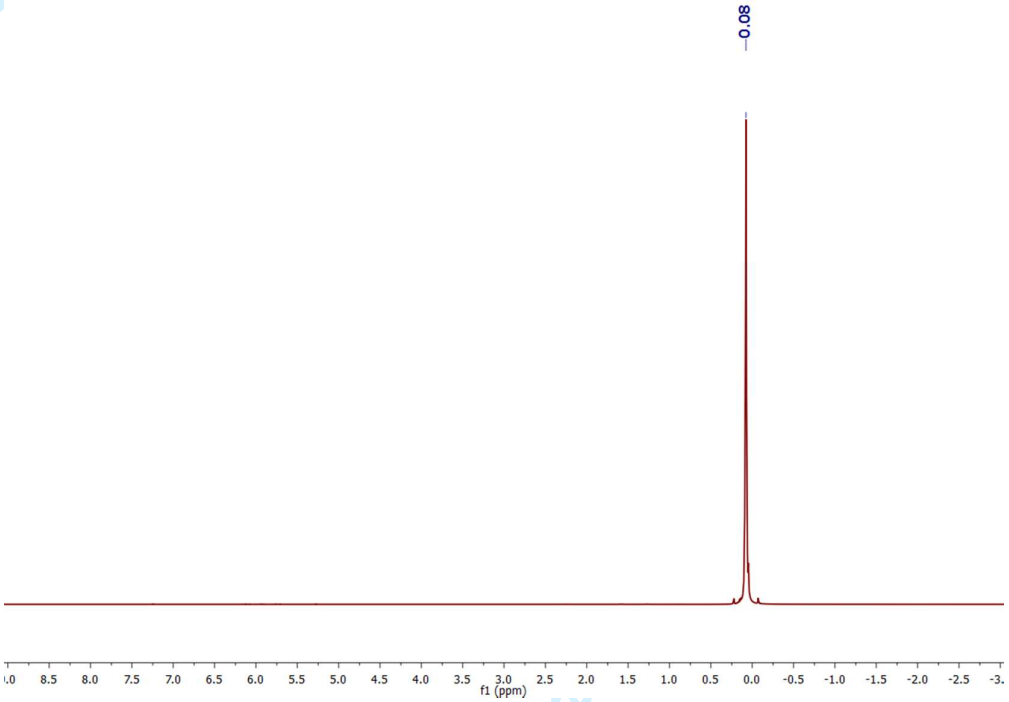

Figure S1c. ^{1}H-NMR spectra of the silicone oil (Polydimethyl Siloxane) in $CDCl_3$.

Table S1. Occurrence of polymorphic forms for the compound *ortho* and *meta*

ortho	**Solvent medium**	**Method**	**Conditions**	**Crystal habit**
Form I	Hexane	Slow evaporation	RT(25-28 °C)	Large plates/needles
	Isooctane, DCM*	Slow evaporation	LT (6 °C)	
Form II	Ethanol*	Slow evaporation	RT (25-28 °C)	Block type plates
	DMSO-DCM	Slow evaporation	RT (25-28 °C)	
meta				
Form I	Hexane	Slow evaporation	RT(25-28 °C)	Blocks
Form II	Toluene	Slow evaporation	LT (4 °C)	Long plates

* SCXRD data were collected for Crystal.

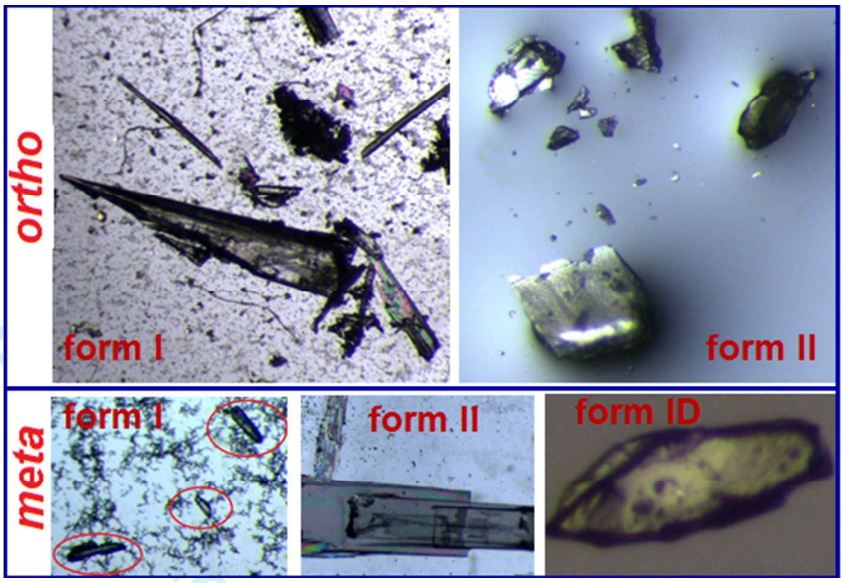

Figure S2. Crystal habits of all polymorphic forms for the compounds *ortho* and *meta*.

Single Crystal X-ray Diffraction (SCXRD), Structure Solution and Refinement

Unit cell measurement, data collection, integration, scaling and absorption corrections for the crystal were done using Bruker Apex II software.[1] Data reduction was done by Bruker SAINT Suite.[2] The crystal structures were solved by direct methods using either by SIR 92[3] or by SIR 2014[4] and refined by the full matrix least squares method using SHELXL 2014[5] present in the program suite WinGX (version 2014.1)[6]. Absorption correction was applied using SADABS.[7] All non-hydrogen atoms were refined anisotropically and all hydrogen atoms were positioned geometrically [HFIX 43 for C(sp^2), N and HFIX 163 for C(sp)] and refined using a riding model. In case of *meta*-**Form ID,** fluorine atom is positional disordered over two *meta* positions of phenyl ring and refined with 54% and 46% occupancy. ORTEPs were generated using Mercury 3.8 (CCDC) program.[8] Geometrical calculations were done using PARST[9] and PLATON.[10]

Table S2. **Crystallographic and refinement data of the polymorphs of *ortho* and *meta***

Data	*ortho*		*meta*		
	Form I	**Form II**	**Form I**	**Form II**	**Form ID**
Formula	$C_{15}H_{10}FNO$	$C_{15}H_{10}FNO$	$C_{15}H_{10}FNO$	$C_{15}H_{10}FNO$	$C_{15}H_{10}FNO$
Formula weight	239.24	239.24	239.24	239.24	239.24
CCDC number	1555054	1555056	1555052	1555055	1555053
Crystal system	monoclinic	monoclinic	monoclinic	monoclinic	monoclinic
Space group	$P2_1/n$	$P2_1/c$	Cc	$P2_1/c$	$P2_1/c$
***a* (Å)**	6.6598(5)	7.2107 (4)	10.8784(9)	13.247(3)	10.8811(15)
***b* (Å)**	10.9338(9)	25.0585 (16)	12.8030(11)	8.8165(19)	12.9584(17)
***c* (Å)**	16.0568 (13)	13.0729 (8)	8.3249(7)	10.389(3)	8.3103(9)
***β* (°)**	93.120(4)	104.3620 (10)	90.136(5)	104.582(9)	90.099(5)
V(Å^3)	1167.47 (16)	2288.3(2)	1159.46(17)	1174.3(5)	1171.8(3)
***Z′*, Z**	1, 4	2, 8	1, 4	1, 4	1, 4
Density (g cm^{-3})	1.361	1.389	1.371	1.353	1.356
F (000)/ *μ* (mm^{-1})	496/ 0.097	992/ 0.099	496/ 0.097	496/ 0.096	496/0.096
θ (min, max)	2.54, 27.31	2.92, 29.51	3.182, 30.526	2.804, 29.809	2.444, 29.130
$h_{min,\ max}$, $k_{min,\ max}$, $l_{min,\ max}$	-8 8, -14 14, -20, 20	-8 8, -29 29, -15, 15	-15 15, -18 18, -11 11	-18 18, -12 12, -14 14	-13 14, -17 17, -11 9
No. of ref.	26240	23773	14341	25481	19256
No. of unique ref./ obs. Ref.	2573 / 1942	4033 / 3415	3475 / 2637	3341 / 2500	3128 / 1970
No. parameters	163	325	164	163	131
R_{all}, R_{obs}	0.0720, 0.0477	0.0610, 0.0504	0.0789, 0.0524	0.0717, 0.0474	0.1341, 0.0729
$wR2_{all}$, $wR2_{obs}$	0.1225, 0.1086	0.1189, 0.1139	0.1280, 0.1171	0.1284, 0.1160	0.1769, 0.1525
$\Delta\rho_{min,\ max}$ (eÅ^{-3})	-0.196, 0.335	-0.237, 0.223	-0.266, 0.312	-0.207, 0.298	-0.456, 0.305
G. O. F.	1.065	1.098	1.050	1.033	1.044

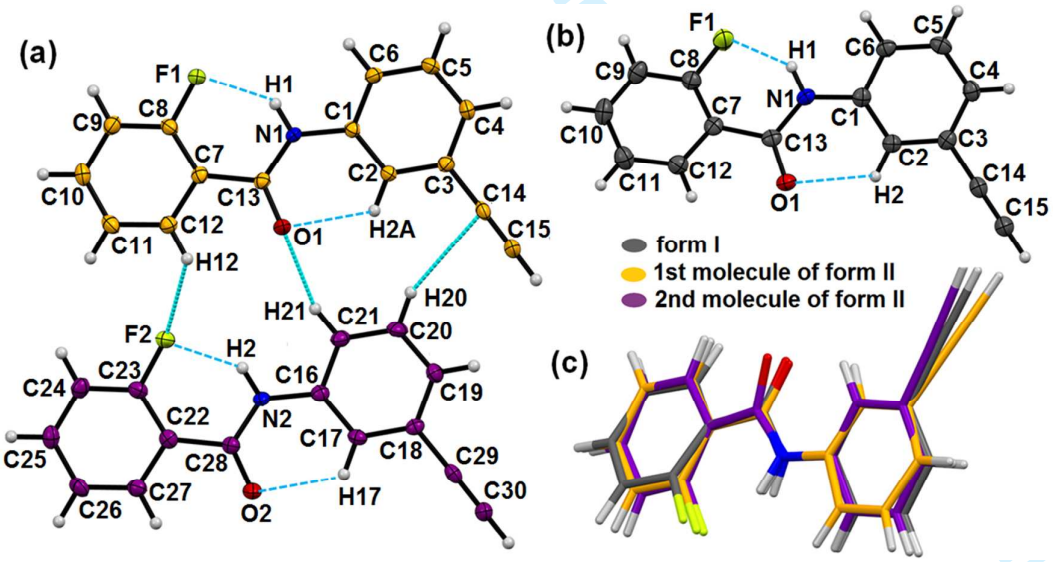

Figure S3. ORTEP (drawn with 50% ellipsoidal probability with the atom numbering scheme) of (a) **Form II** (different colors of carbon atoms showing the symmetry independent molecules) (b) **Form I** for the *ortho* compound. Dotted lines indicates the presence of different intra and intermolecular interactions in the asymmetric unit. (c) Structure overlay

diagram of three molecules (two molecules in the asymmetric unit of **Form II** and one in **Form I)**.

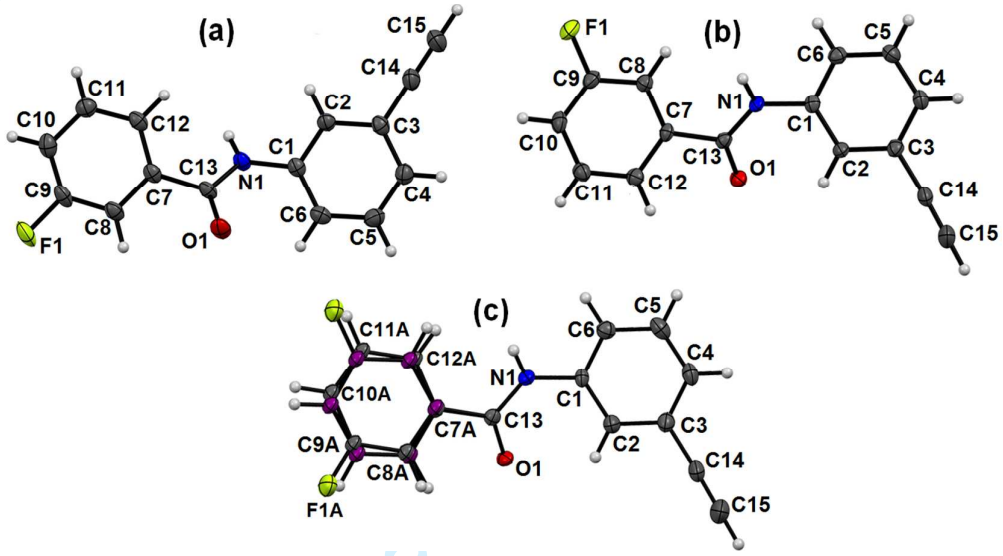

Figure S4. ORTEP (drawn with 50% ellipsoidal probability with the atom numbering scheme.) of (a) *meta*-**Form II** (b) *meta*-**Form I** (c) *meta*-**Form ID** (purple colour of carbon atoms showing minor disorder part).

Phase transition experiment in Silicone oil (SO) at room temperature

Small drop of SO was taken on two separate dry and clean glass slides. After few minutes, to complete the spread over of SO on glass slide, few **Form II** crystals of *ortho* and *meta* were added in SO on two separate glass slides. Then the two glass slides were put under the polarizing optical microscope at room temperature (24-28 °C). After 15-20 minutes needle shaped appearance of **Form I** crystals was observed in case of *ortho* slides. In case of *meta*, the appearance of **Form I** needle crystals from **Form II** was relatively slow. The experiment for *ortho* polymorphs were also repeated in same conditions under Olympus IX83 inverted fluorescence microscope. SCXRD data for the each compound needle shaped **Form I** crystal was collected and listed in Table S4. In case of **Form I** crystal obtained after phase transition **Form II** in SO for *ortho*, the structures were refined as two component non-merohedral twin with HKLF5 dataset. The phase transition experiments in SO were also performed at low temperature (7°C) to very low temperature (-16°C). It has been observed that rate of phase

transition decreases with temperature and at -16°C no transition were found till 4 months. In addition to that we tried these experiments in hydrophilic polymers such as, hexaethylene glycol and poly (diallylamine) instead of SO, but did not observe any phase transition while maintaining the similar conditions.

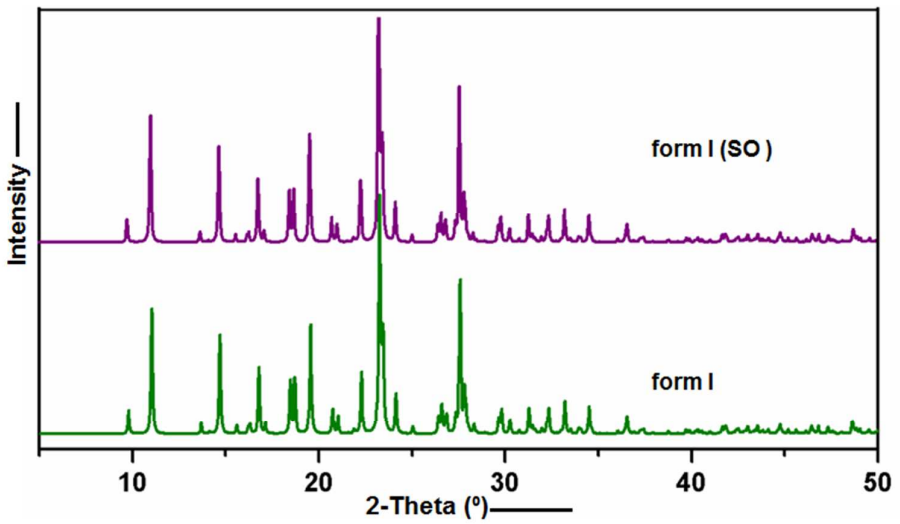

Figure S5. Overlay of simulated PXRD patterns of pure *ortho*-**Form I** crystal and post transition *ortho*-**Form I** crystal obtained in SO from pure *ortho*-**Form II.**

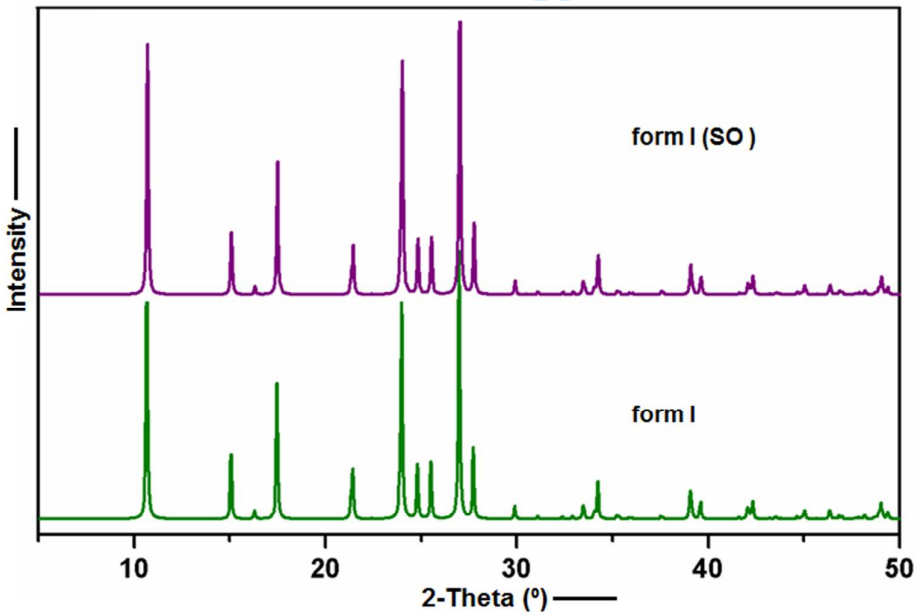

Figure S6. Overlay of simulated PXRD patterns of pure *meta*-**Form I** crystal and post transition *meta*-**Form I** crystal obtained in SO from pure *meta*-**Form II**.

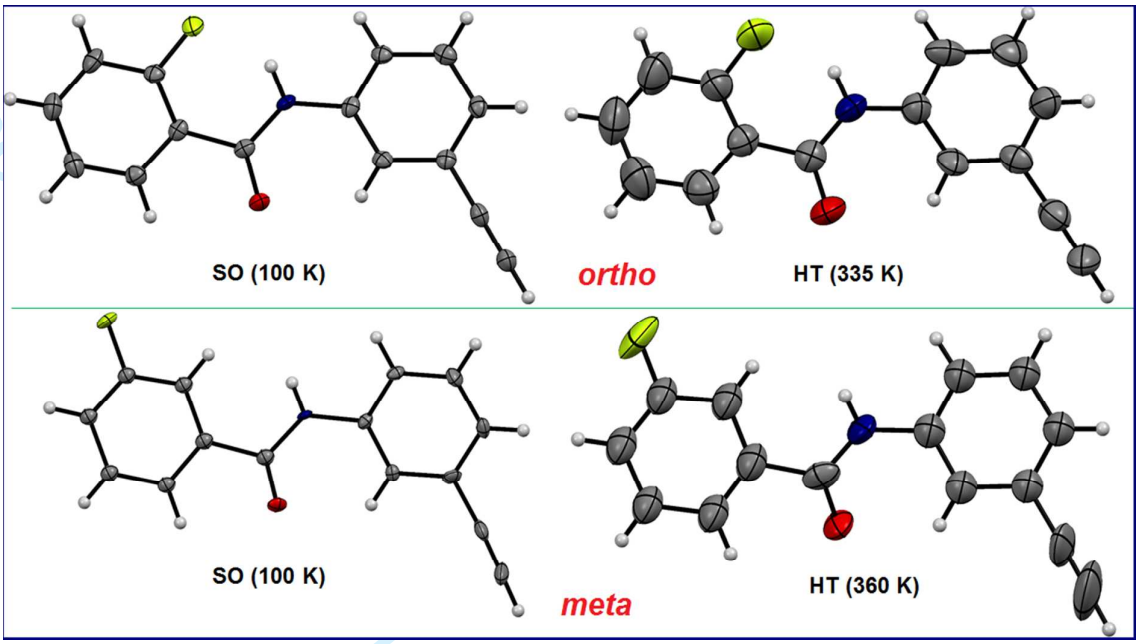

Figure S7. ORTEPS of **Form I** obtained after phase transition from **Form II** crystal in Silicone Oil (SO) as well as high temperature (HT) for both the compound *ortho* and *meta*.

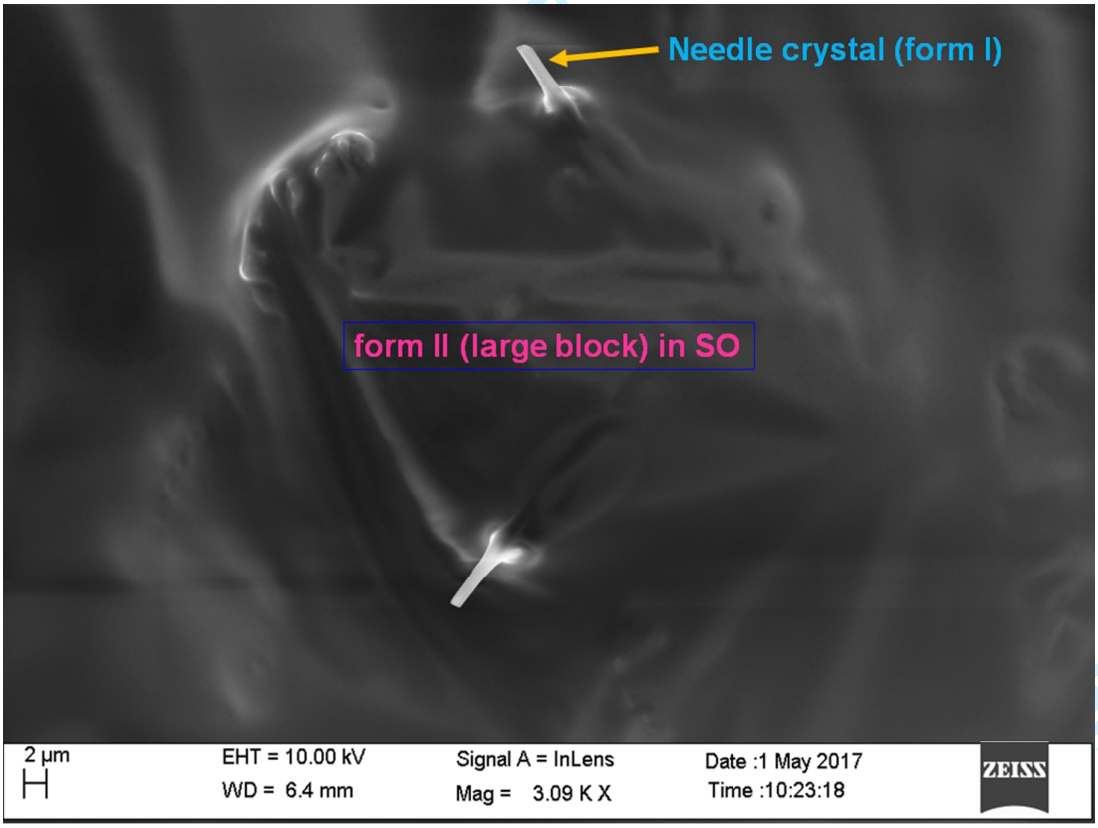

Figure S8. Immediate appearance of needle crystal (**Form I**) on block (**Form II**) crystal in SO of the *ortho* compound in Scanning Electron Microscope (SEM) at RT.

Differential Scanning Calorimetry (DSC) and Microscopy

All DSC experiments were performed using PerkinElmer DSC 6000 instrument under a nitrogen atmosphere in aluminum crucibles. Hot stage microscopy experiments of single crystals were conducted on Linkam LTS420 connected with a Leica polarizing microscope. Silicone oil induced phase transition experiment for *ortho* polymorphs were monitored using Olympus IX83 inverted fluorescence microscope.

Powder X-ray Diffraction (PXRD) and Fourier Transform Infrared Spectroscopy (FTIR)

PXRD patterns of crushed single crystals of all polymorphic forms (**Form I** and **Form II** for each compounds) were performed on a PANalytical Empyrean X-ray Diffractometer with Cu Kα radiation. Diffractograms were collected at room temperature from 0° to 50° with step size of 0.013103° and scan speed- 0.0167 °/sec. Variable-temperature in situ measurements were carried out on crushed **Form II** single crystals for each of the compounds with very slow heating/cooling rate using the *Anton Paar* cryo system and settled down the sample at the temperature of interest to 30 minutes before the each scan. Solid-state FTIR spectra of polymorphic forms (**Form I** and **Form II**) for both compounds were recorded by making thin pellet of crushed crystals with dry potassium bromide in Perkin Elmer instrument at room temperature.

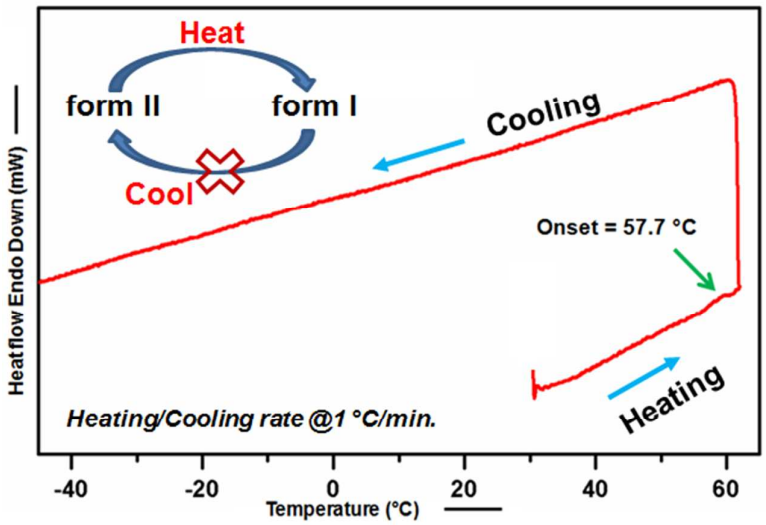

Figure S9. Monotropic irreversible conversion of *ortho*-**Form II** to *ortho*-**Form I** phase at 57.7 °C during heating in DSC.

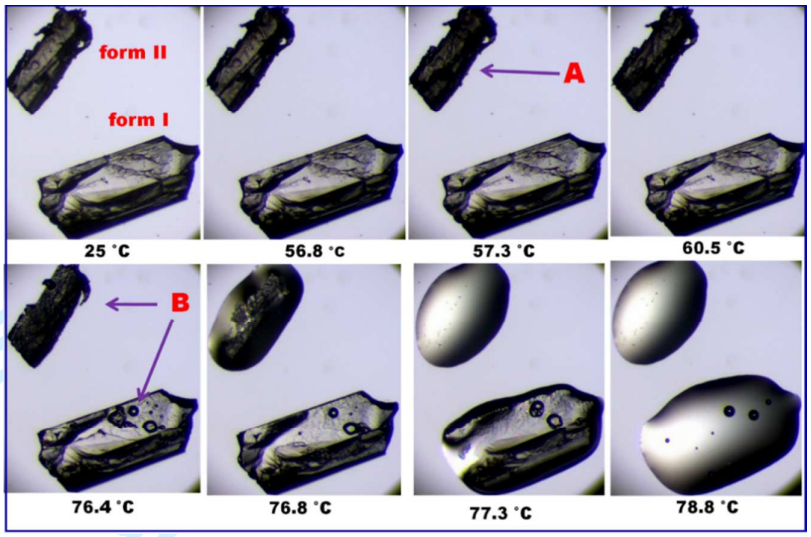

Figure S10. Hot stage microscopy of dimorphs of *ortho* at *1°C/min* heating rate. (A) Solid-to-solid phase transition (crystal became cloudy) from *ortho*-**Form II** to *ortho*-**Form I** at 57.3 °C. (B) Initiation of melting of both the forms at same temperature. Purple arrows showing initiation of phase transitions.

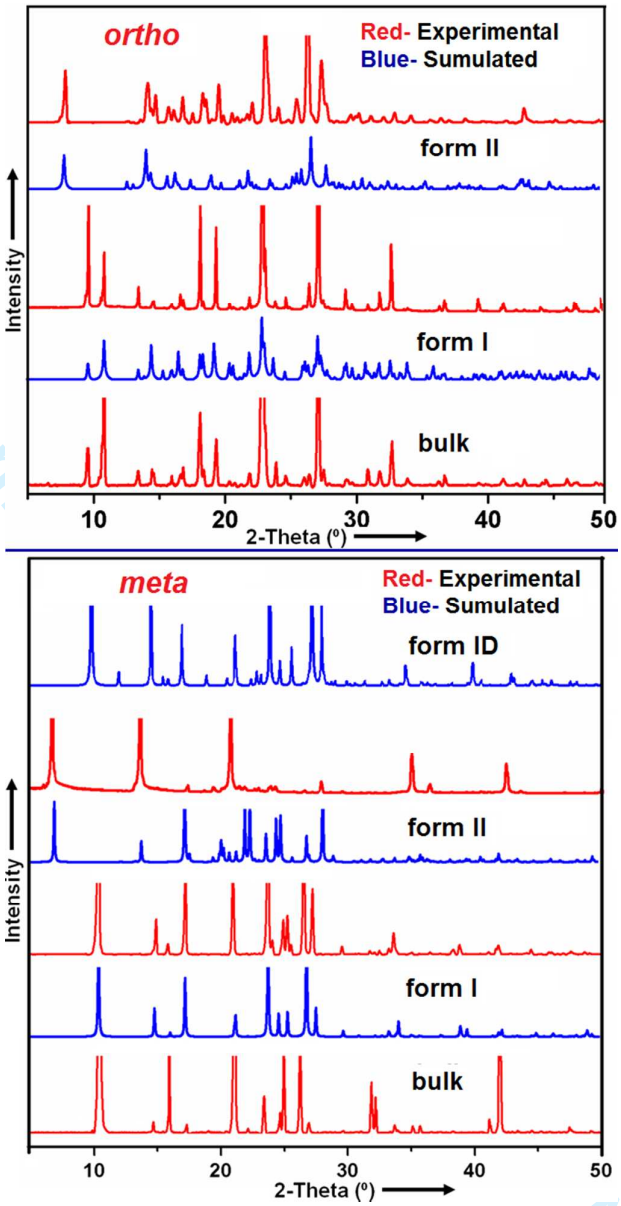

Figure S11. Overlay of experimental (at 298 K, room temperature) and simulated PXRD patterns of two polymorphs (**Form I** and **Form II**) of *ortho* and three polymorphs (**Form I**, **Form II** and **Form ID**) of *meta* including bulk powder compounds. Experimental PXRD patterns of *meta*-**Form ID** was not recorded due to lack of crystals.

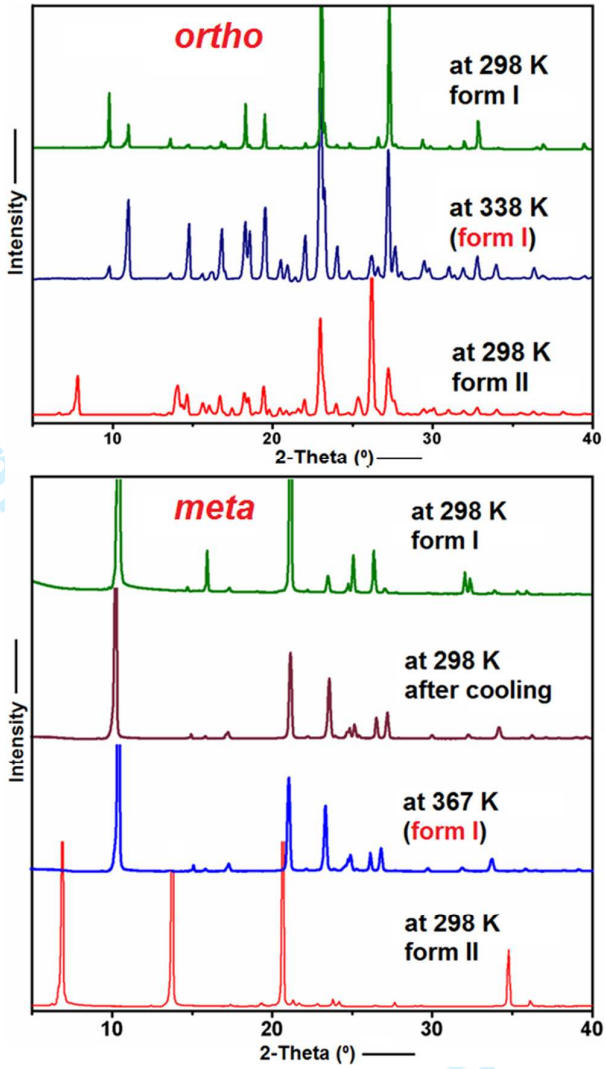

Figure S12. Variable temperature PXRD patterns of **Form II** for *ortho* (above) and *meta* (below) polymorphs. Green patterns (at the top) showing experimental PXRD of pure **Form I** phase at room temperature (298K) for comparison purposes.

Temperature induced Single-Crystal-to-Single-Crystal phase transition experiment in SCXRD instrument

A small good quality single crystal of **Form II** was mounted in Bruker D8 Venture instrument equipped with Oxford cryo-system at room temperature for *ortho* and *meta* polymorphs in separate two experiments. At first, unit cell was measured at room temperature (294 K). Then the temperature was gradually increased (Ramp rate- 50 K/hr. for *ortho* and 80 K/hr. for *meta*) by cryo-system for a particular fixed position of mounted **Form II** crystal in loop. When the temperature of the cryo-system reached at 335 K for *ortho* and 360 K for *meta*, the crystal was held for one and half an hour to ensure complete

conversion from **Form II** to **Form I**. To ensure about the complete phase transition the unit cell was measured and during this occasion the crystal fell down from the cryo loop. This may be happens because of the phase transition. The cryo oils were not used to fix the crystal in cryo loop because the presence of cryo oil or glue can affect the phase transition (as phase transition was also observed in silicone oil). After several attempts with a new single crystal we succeeded to collect single crystal data at 335 K for *ortho* and 360 K for *meta* for the mounted crystal after the phase transition. The quality of crystal at high temperature decreases after phase transition and a few ill-defined reflections were found after the phase transition in reciprocal lattice and these reflections have been separated from the actual domain. Then with this domain HKLF4 dataset, the crystal structures were solved followed by refinements (see above). After that it has been confirmed that **Form II** crystal was almost completely converted to **Form I** at high temperature.

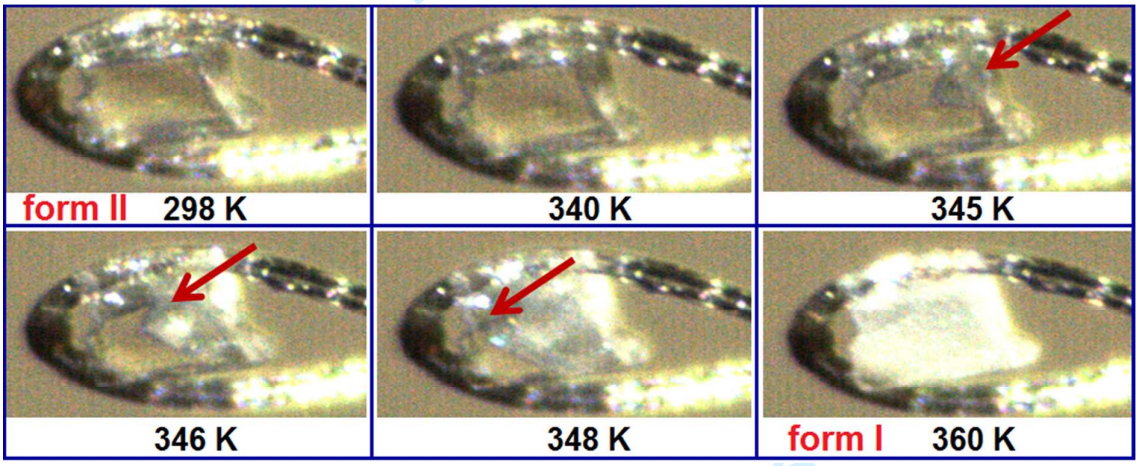

Figure S13. Propagation of crystal interface during heating on *meta*-**Form II** crystal in SCXRD instrument. Red arrows showing the displacement of phase front (*meta*-**Form I**) at different temperature.

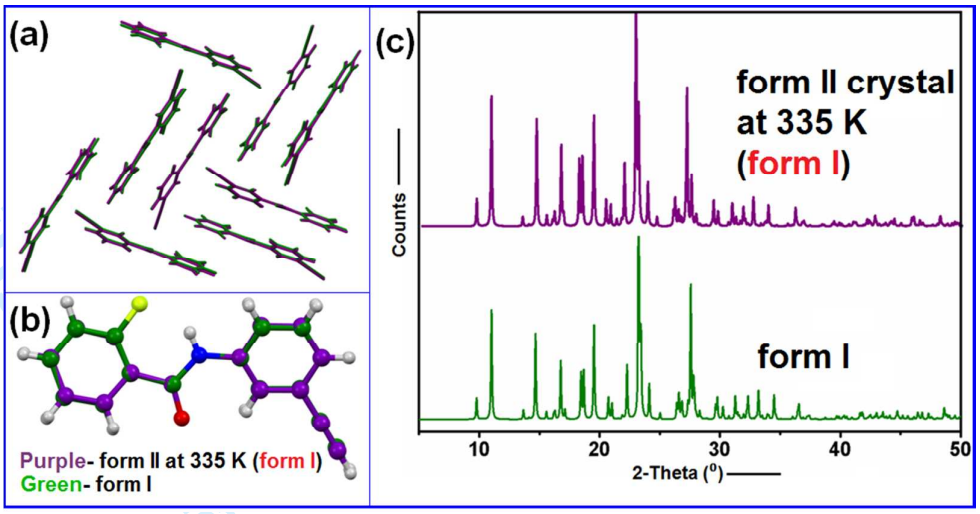

Figure S14. (a) Packing overlay of molecules **(b)** Overlay of molecules in asymmetric unit and **(c)** Simulated PXRD patterns of pure **Form I** crystal and **Form II** crystal after phase transition to **Form I** at 335K in *ortho* polymorphs.

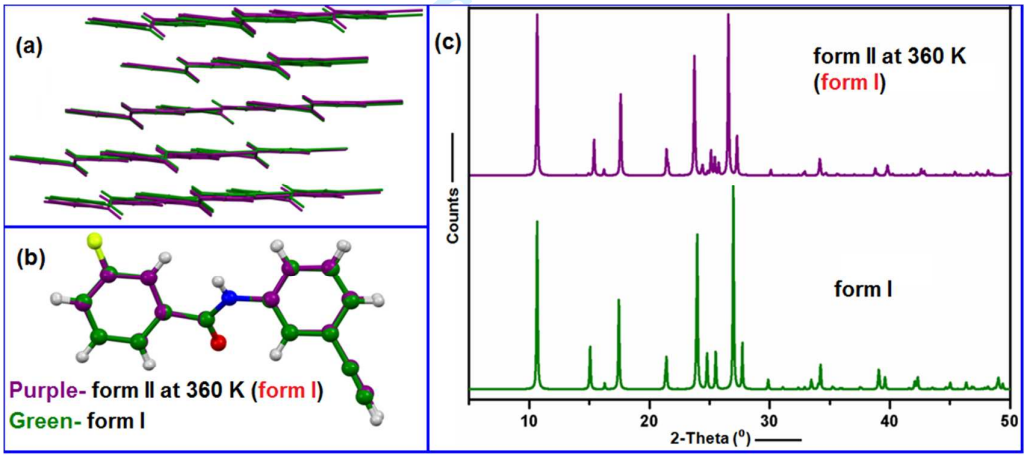

Figure S15. (a) Packing overlay of molecules **(b)** Overlay of molecules in asymmetric unit. **(c)** Simulated PXRD patterns of pure **Form I** crystal and **Form II** crystal after phase transition to **Form I** at 360K in *meta* polymorphs.

Table S3. Crystallographic and refinement data of the Form I polymorphs obtained after phase transition from Form II in silicone oil (SO) and high temperature (HT) of *ortho* and *meta*.

Data	*ortho*		*meta*	
	Form I (SO)	**Form I (HT)**	**Form I (SO)**	**Form I (HT)**
Formula	$C_{15}H_{10}FNO$	$C_{15}H_{10}FNO$	$C_{15}H_{10}FNO$	$C_{15}H_{10}FNO$
Formula weight	239.24	239.24	239.24	239.24
Temperature (K)	100(2)	335(2)	100(2)	360(2)
Crystal system	monoclinic	monoclinic	monoclinic	monoclinic
Space group	$P2_1/n$	$P2_1/n$	Cc	Cc
***a* (Å)**	6.6404(13)	6.710(8)	10.878(3)	11.18(3)
***b* (Å)**	10.909(2)	11.125(14)	12.806(4)	13.01(4)
***c* (Å)**	16.016(13)	16.352(19)	8.329(2)	8.43(3)
***β* (˚)**	93.136(7)	93.55(4)	90.169(11)	92.29(7)
V(Å^3)	1158.5 (4)	1218(2)	1160.4(6)	1224(6)
***Z′*, Z**	1, 4	1, 4	1, 4	1, 4
Density (g cm^{-3})	1.372	1.304	1.369	1.298
F (000)/ *μ* (mm^{-1})	496/ 0.097	496/ 0.93	496/ 0.097	496/ 0.092
θ (min, max)	2.60, 24.999	2.216, 28.282	2.457, 27.875	2.404, 26.371
$h_{min, max}$, $k_{min, max}$, $l_{min, max}$	-7 7, -12 12, 0 18	-8 8, -11 14, -21 21	-14 14, -16 16, -10 10	-12 13, -16 16, -10 10
No. of ref.	2016	9761	7210	4782
No. of unique ref./ obs. Ref.	2016 / 1492	2985 / 656	2488 / 1293	2257 / 734
No. parameters	164	167	128	104
R_{all}, R_{obs}	0.0953, 0.0630	0.4960, 0.1651	0.2051, 0.0904	0.3568, 0.1275
$wR2_{all}$, $wR2_{obs}$	0.1566, 0.1435	0.2680, 0.1788	0.1461, 0.1171	0.2549, 0.1874
$\Delta\rho_{min, max}$ (eÅ^{-3})	-0.380, 0.284	-0.214, 0.191	-0.389, 0.417	-0.208, 0.296
G. O. F.	1.110	0.976	1.022	1.011

Table S4. List of Selected Torsion Angles for *ortho* and *meta* Polymorphs

	ortho		*meta*		
Torsions (in degree)	**Form I**	**Form II**	**Form I**	**Form II**	**Form ID**
T_1 (C12-C7-C13-N1 / C27-C22-C28-N2)	-168.81(2) NA	176.1(2) /-168.4(2)	-149.0(2) NA	-33.8(2) NA	38.7(4) NA
T_2 (C7-C13-N1-C1 / C22-C28-N2-C16)	178.39(2) NA	-179.8(2) /178.0(2)	-179.5(2) NA	175.8(1) NA	178.8(3) NA
T_3 (C6-C1-N1-C13 / C21-C16-N2-C28)	-162.34(2) NA	-174.8(2) /177.86(2)	145.4(3) NA	35.4(2) NA	147.1(2) NA

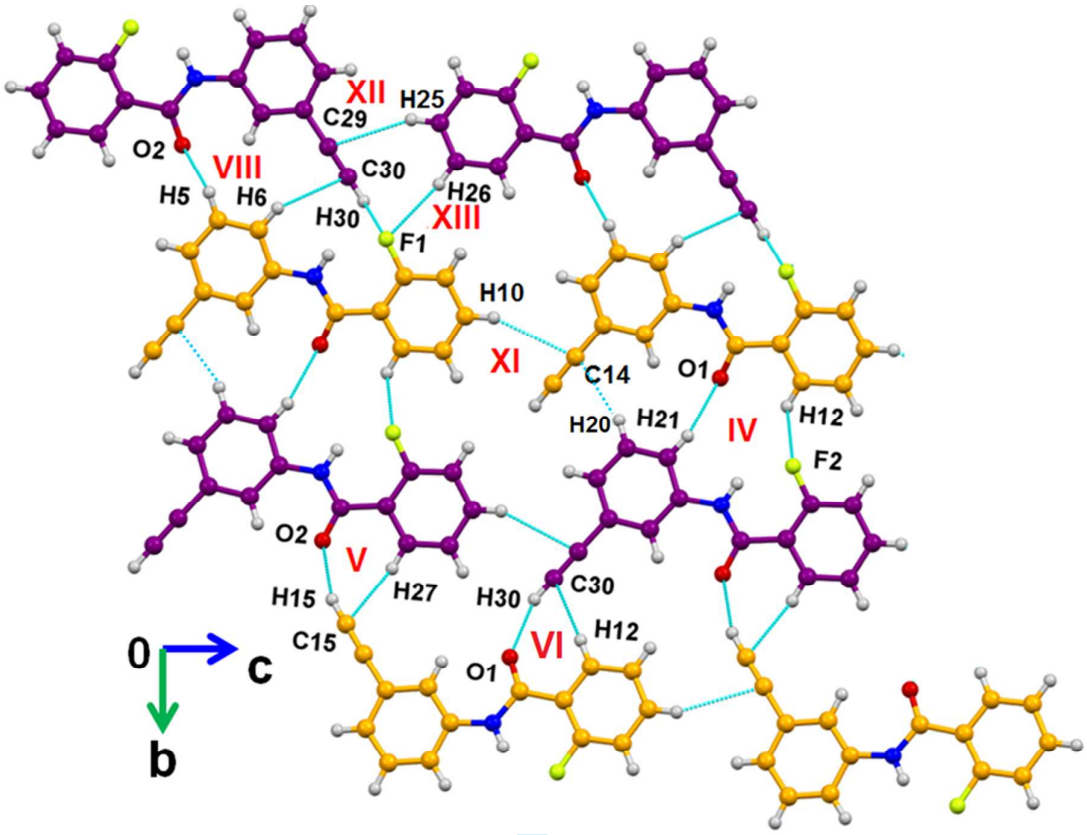

Figure S16. Formation of molecular sheet in the crystal packing of *ortho*-**Form II** polymorph stabilized by C(sp^2/sp)-H···O, C(sp^2/sp)-H···F and C-H(sp^2)···π(triple bond/ring) interactions.

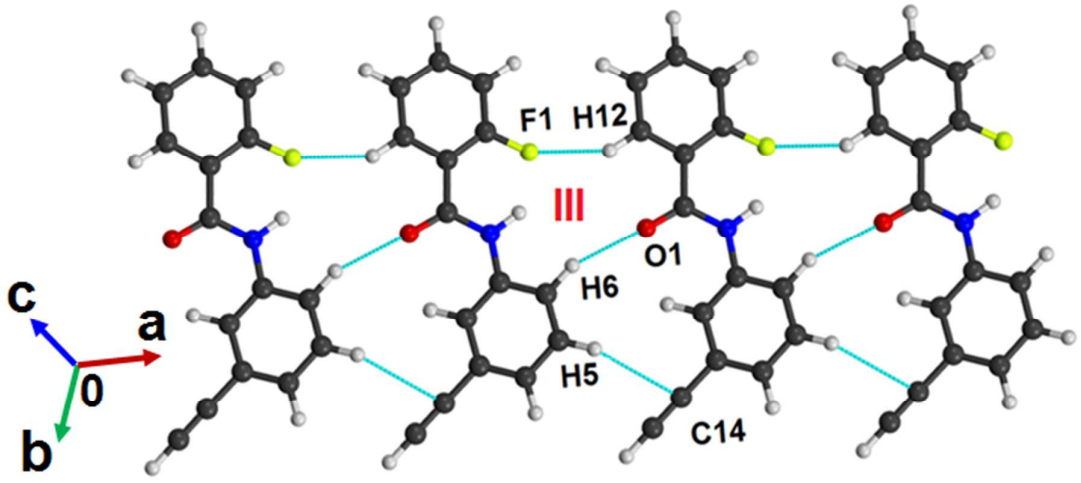

Figure S17. Formation of molecular sheet in the crystal packing of *ortho*-**Form I** polymorph via C(sp^2)-H···O, C(sp^2)-H···F and C-H(sp^2)···π(triple bond/ring) interactions.

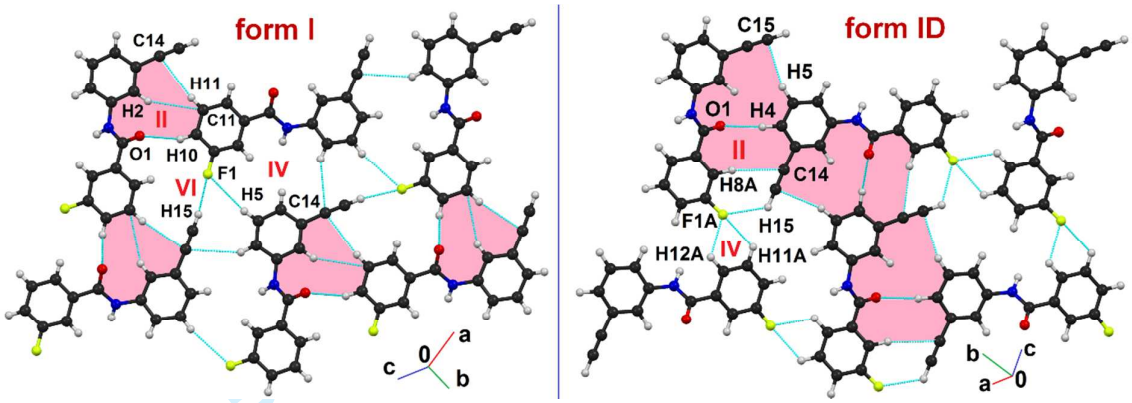

Figure S18. Formation of molecular sheets in the crystal packing of *meta*-**Form I** and *meta*-**Form ID** polymorphs stabilized by C(sp^2)-H···O, C(sp^2/sp)-H···F and C-H···π(triple bond/ring) interactions.

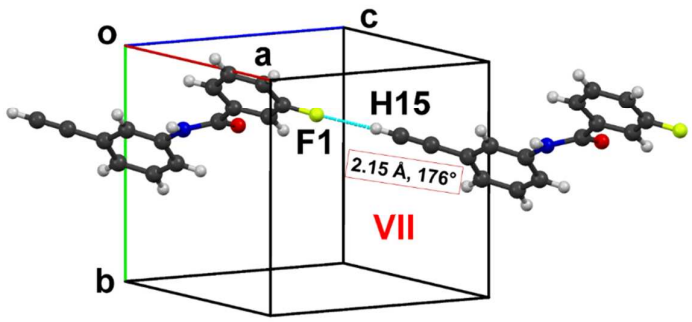

Figure S19. Formation of very short and highly directional C-H···F hydrogen bond (motif VII) in the crystal packing of *meta*-**Form II.**

Theoretical Calculations

Lattice energy (polymorphs) and intermolecular interaction energy (of selected molecular pairs) with its decomposition into their coulombic, polarization, dispersion and repulsion contributions for the all polymorphs were calculated by the PIXEL method. Initially, hydrogen atoms were moved to their neutron values and molecular electron density were obtained at MP2/6-31G** with Gaussian 09.[11] The PIXEL calculation for *meta*-**Form ID** was performed considering major disorder part (A part). Results obtained from the PIXEL

was found comparable with high-level MP2 and DFT-D quantum mechanical calculations (References [33-35] in main manuscript).

Table S5. Intra- and intermolecular Interactions along with interaction energies (I.E. in kJ/mol) obtained from the PIXEL method

Motifs	Symmetry	distance (Å)	E_{Coul}	E_{Pol}	E_{Disp}	E_{Rep}	E_{Tot}	Possible Interactions	Geometry (Å/ º)
	ortho Form I ($P2_1/n$ Z'=1)								
I	2-x, -y, 1-z	4.303	-7.5	-6.3	-48.9	31.0	-31.7	π(C2/C3/C14)...π(C11/C12)	3.516 (2)
II	1-x, -y, 1-z	5.464	-9.2	-3.1	-36.0	19.3	-29.0	(C5)π...π(C8) C6-H6...N1	3.485 (2) 2.90, 120
III	1+x, y, z	6.660	-10.4	-4.4	-23.1	15.3	-22.5	C6 -H6 ...O1 C12-H12...F1 C5-H5...π(C14/C15)	2.42, 150 2.51, 128 2.88, 134
IV	2-x, 1-y, 1-z	9.025	-4.9	-1.1	-19.3	9.9	-15.4	(C9)π...π(C11)	3.655 (3)
V	3/2-x, -1/2+y, 3/2-z	7.956	-1.9	-2.3	-20.0	11.0	-13.2	(C15)π...π(C6/C1)	3.487 (2)
VI	5/2-x, 1/2+y, 3/2-z	9.513	-15.5	-5.8	-9.9	19.1	-12.1	C15-H15...O1	2.08, 170
VII	-1/2+x, 1/2-y, 1/2+z	9.313	-4.3	-2.0	-12.4	7.7	-10.9	C10-H10.... π(C4/C5)	2.71, 151
VIII	1/2+x, 1/2-y, 1/2+z	8.995	-5.7	-1.6	-9.4	6.0	-10.7	C9-H9... π(C14) C10-H10... π(C15)	3.02, 134 2.93, 125
IX	1-x, 1-y, 1-z	9.633	-1.6	-0.5	-6.6	1.7	-6.9	C9-H9...F1	2.78, 131
X	x, y, z							N1-H1...F1(intra) C2-H2...O1(intra)	1.88, 135 2.25, 115
	ortho Form II ($P2_1/c$ Z'=2)							Cg1- C1> C6, Cg2- C7> C12, Cg1'-C16>C21, Cg2'-C22>C27	
I (a...a)	1-x, -y, 2-z	3.862	-15.4	-6.2	-63.9	47.7	-37.7	Cg1(C1>C6)...Cg2(C7>C12)	3.765 (3)
II (a...a)	2-x, -y, 2-z	5.255	-13.4	-4.3	-50.1	32.2	-35.6	(C1)π... π (C10) (C7)π... π(C7)	3.394 (3) 3.527 (3)
III (b...b)	x, 1/2-y, -1/2+z	6.546	-9.3	-4.9	-44.5	32.3	-26.4	Cg1'(C16>C21)...Cg2'(C22>C27)	3.659 (3)
IV (a...b)	x, y, z	6.540	-8.2	-4.2	-26.1	17.0	-21.5	C21 -H21 ...O1 C20-H20...π (C14) C12-H12...F2	2.44, 144 2.92, 148 2.66, 113
V (a...b)	-1+x, 1/2-y, -1/2+z	9.719	-18.8	-5.9	-13.0	18.4	-19.3	C15-H15...O2 C27-H27... π (C15)	2.19, 154 2.68, 140
VI (a...b)	x, 1/2-y, -1/2+z	9.564	-16.9	-5.1	-12.2	15.3	-18.9	C30-H30...O1 C12-H12... π (C30)	2.63, 143 2.68, 154
VII (a...b)	2-x, -y, 2-z	6.893	-5.4	-3.4	-23.3	14.0	-18.1	C6-H6 ...F2 F1...F2 C9-H9... π (C21)	2.80, 145 2.99 (2) 2.90, 139
VIII (a...b)	1-x, 1/2+y, 3/2-z	7.931	-5.5	-3.0	-20.6	11.6	-17.5	C30 -H30...F1 C5-H5...O2 C6-H6... π (C14/C15)	2.63, 119 2.71, 124 2.89, 131
IX (b...b)	-1+x, 1/2-y, -1/2+z	8.453	-3.7	-2.0	-24.9	14.6	-15.9	Cg1' (C16>C21)...Cg2'(C22>C27)	3.742 (3)
X	1-x, -y, 1-z	9.993	1.9	-1.1	-12.2	3.2	-8.1	(C4)π... π(C14)	3.799 (3)

(a...a)									
XI (a...a)	-1+x, y, -1+z	13.272	-2.9	-2.3	-12.0	9.5	-7.7	C10-H10... π (C14/C15)	2.77, 142
XII (b...b)	x+1, y, z+1	13.272	-3.1	-2.4	-11.8	9.7	-7.7	C25-H25... π (C29/C30)	2.77, 141
XIII (a...b)	2-x, -1/2+y, 5/2-z	10.609	-1.3	-0.8	-8.1	2.9	-7.2	C26-H26...F1	2.64, 150
XIV (a...a)	-x, -y, 1-z	12.016	-0.5	-0.9	-9.7	4.0	-7.1	(C4)π...π(C15)	3.668 (3)
XV (a...b)	1-x, -y, 1-z	12.058	-0.8	-0.2	-4.9	0.9	-5.1	H5...H19 (dispersive)	-
XVI	x, y, z							N1-H1...F1 (intra) N2-H2 ...F2 (intra) C2-H2A...O1 (intra) C17-H17...O2 (intra)	1.88, 137 1.89, 135 2.18, 118 2.19, 118
	meta Form I (*C c* Z'=1)								
I	x, -y, z+1/2	4.172	-46.5	-18.5	-55.7	68.1	-52.6	N1-H1⋯O1 (C12)π⋯π(C5/C6) (C8)π⋯π(C13)	1.85, 160 3.404(3) 3.374(3)
II	x-1/2, -y-1/2, z+1/2	9.191	-7.4	-4.6	-20.9	16.0	-16.9	C10-H10⋯O1 C2-H2⋯π(C11) C11-H11⋯π(C14)	2.56, 133 3.00, 153 2.81, 170
III	x+1/2, y+1/2, z	8.400	-4.0	-3.3	-24.2	18.2	-13.3	(C11/C12)π⋯π(C5/C6)	3.449(3)
IV	x-1/2, -y+1/2, z+1/2	9.575	-1.6	-3.1	-17.7	10.2	-12.4	C6-H6⋯π(C15/C14) C5-H5⋯F1	2.96, 150 2.86, 163
V	x-1/2, y-1/2, z+1	11.836	-2.9	-0.8	-10.3	3.7	-10.3	C4-H4⋯π(C10)	3.15, 119
VI	x-1, y, z+1	13.714	-4.5	-1.2	-3.8	4.3	-5.1	(*sp*)C15-H15⋯F1	2.26, 167
	meta Form II ($P2_1/c$ Z'=1)								
I	x, -y+1/2, z+1/2	5.199	-32.0	-11.5	-34.5	32.2	-45.8	N1-H1⋯O1 C8-H8⋯ π(C11) C2-H2⋯ π(C6) C12-H12⋯O1	2.08, 160 2.74, 174 2.95, 163 2.59, 127
II	-x+1, -y, -z	4.692	-17.4	-5.4	-46.8	29.6	-40.1	(C11)π⋯π(C1) (C10)π⋯π(C2)	3.500(2) 3.539(2)
III	-x+1, -y+1, -z	4.262	-7.2	-3.4	-45.5	28.9	-27.1	(C5)π⋯π(C8/C9)	3.355(2)
IV	-x+1, y-1/2, -z-1/2	6.925	-5.1	-3.8	-17.4	14.4	-11.9	C10-H10⋯π(C15) C11-H11⋯π(C2/C3)	2.92, 132 2.70, 163
V	-x+1, y-1/2, -z+1/2	6.789	-5.6	-3.0	-15.2	12.9	-10.8	C5-H5⋯F1 C5-H5⋯π(C9)	2.30, 160 2.71, 139
VI	x-1, -y+1/2, z -1/2	12.956	-0.8	-1.0	-8.7	4.3	-6.2	C10-H10⋯π(C15)	2.98, 115
VII	x-1, y, z-1	14.633	-6.0	-1.8	-4.4	7.0	-5.2	(*sp*)C15-H15⋯F1	2.15, 176
VIII	-x, y-1/2, -z-1/2	12.975	-0.5	-0.5	-5.0	1.7	-4.3	C4-H4⋯π(C15)	3.07, 137
	meta Form ID (($P2_1/c$ Z'=1) Cg2= C7A>C12A								
I	x, -y+1/2, z-1/2	4.263	-74.3	-25.6	-56.3	122.1	-34.2	N1-H1...O1 (C1)π⋯π(C7A) (C6)π⋯π(C8A) (C2)π⋯π(C15)	1.86, 161 3.5485(3) 3.4305(3) 3.5520(3)
II	-x+1, y+1/2, -z+1/2	8.823	-15.9	-6.7	-23.3	30.8	-15.1	C4-H4...O1 C15-H15...F1A C5-H5… π(C14/C15) C8A-H8A… π(C14/C15)	2.64, 144 2.55, 122 2.84, 175 2.71, 156
III	-x, -y, -z+1	8.184	-24.5	-7.2	-27.0	47.1	-11.6	(Cg2)π⋯π(Cg2)	3.824(*)
IV	-x, y-1/2, -z+3/2	10.080	-3.3	-3.0	-13.3	11.8	-7.7	C12A-H12A… π(C9A/C10A) C11A-H11A…F1A C12A-H12A…F1A	3.31, 154 2.68, 137 2.59, 120

V	-x+1, -y+1, -z	11.712	-4.2	-1.5	-9.9	9.1	-6.5	C4-H4... π(C4) C4-H4... π(C14)	3.43, 115 3.47, 114
VI	-x, -y, -z+2	12.159	-5.1	-1.6	-7.9	8.5	-6.0	C10A-H10A… π(C11A/C10A)	3.16, 125
VII	x-1, -y+1/2, z+1/2	11.693	-2.0	-0.6	-3.6	3.0	-3.2	C11A-C15	3.9540(4)

REFERENCES

1. Apex2, Version 2 User Manual, M86-E01078, Bruker Analytical X-ray Systems Madison, WI, 2006.

2. Siemens, SMART System, Siemens Analytical X-ray Instruments Inc. Madison, MI, 1995.

3. Altomare, A.; Cascarano, G.; Giacovazzo, C.; Guagliardi, A. *J. Appl. Crystallogr.* **1994**, *27*, 435.

4. Burla, M. C.; Caliandro, R.; Carrozzini, B.; Cascarano, G. L.; Cuocci, C.; Giacovazzo, C.; Mallamo, M.; Mazzone, A.; Polidori, G. *J. Appl. Crystallogr.* **2015**, *48*, 306.

5. Sheldrick, G. M. *Acta Crystallogr.* **2015**, *C71*, 3.

6. Farrugia, L. J. *J. Appl. Crystallogr.* **1999,** *32*, 837.

7. Sheldrick, G. M. SADABS; Bruker AXS, Inc.: Madison, WI, 2007.

8. Macrae, C. F.; Bruno, I. J.; Chisholm, J. A.; Edgington, P. R.; McCabe, P.; Pidcock E.; Rodriguez-Monge, L.; Taylor, R.; Streek, J.; Wood, P. A. *J. Appl. Crystallogr.* **2008**, *41*, 466.

9. Nardelli, M. *J. Appl. Crystallogr.* **1995**, *28*, 659.

10. Spek, A. L. *Acta Crystallogr.* **2009**, *D65*, 148.

11. Frisch, M. J.; Trucks, G. W.; Schlegel, H. B.; Scuseria, G. E.; Robb, M. A.; Cheeseman, J. R.; Scalmani, G.; Barone, V.; Mennucci, B.; Petersson, G. A.; Nakatsuji, H.; Caricato, M.;

Li, X.; Hratchian, H. P.; Izmaylov, A. F.; Bloino, J.; Zheng, G.; Sonnenberg, J. L.; Hada, M.; Ehara, M.; Toyota, K.; Fukuda, R.; Hasegawa, J.; Ishida, M.; Nakajima, T.; Honda, Y.; Kitao, O.; Nakai, H.; Vreven, T.; Montgomery, J. A., Jr.; Peralta, J. E.; Ogliaro, F.; Bearpark, M.; Heyd, J. J.; Brothers, E.; Kudin, K. N.; Staroverov, V. N.; Kobayashi, R.; Normand, J.; Raghavachari, K.; Rendell, A.; Burant, J. C.; Iyengar, S. S.; Tomasi, J.; Cossi, M.; Rega, N.; Millam, J. M.; Klene, M.; Knox, J. E.; Cross, J. B.; Bakken, V.; Adamo, C.; Jaramillo, J.; Gomperts, R.; Stratmann, R. E.; Yazyev, O.; Austin, A. J.; Cammi, R.; Pomelli, C.; Ochterski, J. W.; Martin, R. L.; Morokuma, K.; Zakrzewski, V. G.; Voth, G. A.; Salvador, P.; Dannenberg, J. J.; Dapprich, S.; Daniels, A. D.; Farkas, Ö.; Foresman, J. B.; Ortiz, J. V.; Cioslowski, J.; Fox, D. J. *Gaussian 09, Revision A.02*, Gaussian, Inc., Wallingford CT, **2009.**